

# Description of light clusters in relativistic nuclear models

Márcio Ferreira and Constança Providência  
*Centro de Física Computacional, Department of Physics,  
University of Coimbra, P-3004-516 Coimbra, Portugal*

Light clusters are included in the equation of state of nuclear matter within the relativistic mean field theory. The effect of the cluster-meson coupling constants on the dissolution density is discussed. Theoretical and experimental constraints are used to fix the cluster-meson couplings. The relative light cluster fractions are calculated for asymmetric matter in chemical equilibrium at finite temperature. It is found that above  $T = 5$  MeV deuterons and tritons are the clusters in larger abundances. The results do not depend strongly on the relativistic mean field interaction chosen.

PACS number(s): 21.65.+f, 24.10.Jv, 26.60.+c,  
95.30.Tg

## I. INTRODUCTION

To gain a deeper understanding of the physics involved in stellar core collapse, supernova explosion and protoneutron star evolution, an equation of state capable of describing matter ranging from very low densities to few times the saturation density and from zero temperature to a few MeV is needed.

The crust of the star is essentially determined by the low density region of the equation of state (EOS), while the high density part will be important to define properties such as the star mass and radius. Understanding the crust constitution of a neutron star is an important issue because it influences the cooling process of the star and plays a decisive role on quantities such as the neutrino emissivity and gravitational waves emission.

In the outer crust, where the density is lower, the formation of light clusters in nuclear matter will be energetically favorable at finite temperature, as in core-collapse supernovae or neutron star mergers, whereas in catalyzed cold neutron stars only heavy nuclei appear. At very low densities and moderate temperatures, the few body correlations are expected to become important and the system minimizes its free energy by forming light nuclei like deuterons ( $d \equiv {}^2\text{H}$ ), tritons ( $t \equiv {}^3\text{H}$ ), helions ( $h \equiv {}^3\text{He}$ ) and  $\alpha$ -particles ( ${}^4\text{He}$ ) due to the increased entropy [1, 2]. Eventually, these clusters will dissolve at higher densities due to Pauli blocking resulting in an homogeneous matter [2]. In particular, the cooling process of a protoneutron star is affected by the appearance of light clusters [3].

The inclusion of light clusters ( $d$ ,  $h$ ,  $t$  and  $\alpha$  particles) in the nuclear matter EOS is discussed in [1], where the most important thermodynamical quantities are calculated within a density-dependent relativistic model. The conditions for the liquid-gas phase transition are obtained, and it is seen how the binodal section is affected by the inclusion of these clusters. Moreover, an EOS is obtained starting at low densities with clusterized matter up to high density cluster-free homogeneous matter. In this work the density and temperature dependence of the

in-medium binding energy of the clusters was determined within a quantum statistical approach [4] and included in a phenomenological way in the relativistic mean field (RMF) model with density dependent couplings.

The  $\alpha$  particle is the most strongly bound system among all light nuclei and it certainly plays a role in nuclear matter as has been pointed out in [1, 4–7]. Lattimer and Swesty [5] worked out the EOS in the compressible extended liquid drop model based on a non-relativistic framework appropriate for supernova simulations, for a wide range of densities, proton fractions and temperatures, including the contribution of  $\alpha$  particle clusters. An excluded volume prescription is used to model the dissolution of  $\alpha$  particles at high densities. The same is done by H. Shen et al. in [6] where non-uniform matter composed of protons, neutrons,  $\alpha$  particles and a single species of heavy nuclei is described with the Thomas-Fermi approximation and the TM1 parametrization of the non-linear Walecka model (NLWM). At low densities, these particles are described by classical gases.

In [7] the virial expansion of low-density nuclear matter composed by neutrons, protons, and  $\alpha$  particles is presented, and it is shown that the predicted  $\alpha$  particles concentrations differ from the predictions of the EOS proposed in [5] and [6]. The virial expansion was extended to include other light clusters with  $A \leq 4$  [8, 9]. All possible light clusters were also included in recent EOS appropriate for simulations of core-collapse supernovae based in a nuclear statistical equilibrium model, including excluded volume effects for nuclei [10].

The aim of the present work is to study the dissolution density of light clusters, i.e. the density above which light clusters do not exist anymore, in uniform nuclear matter within the framework of the NLWM [11]. The dependence of the dissolution density on the cluster-meson couplings as well as on the proton-fraction will be studied. In many models which include light clusters the dissolution density is determined by excluded volume effects [5, 6, 10]. In Ref. [9], a statistical excluded volume model was compared with two quantum many-body models, a generalized relativistic mean-field model [1] and a quantum statistical model [2, 12]. It was shown that the excluded volume description works reasonably well at high temperatures, partly due to a reduced Pauli blocking. However, at low temperatures the excluded

volume approach shows crucial deviations from the statistical approach.

In [13], using a RMF approach, the coupling of the  $\alpha$ -clusters to the  $\omega$ -meson was employed to describe the dissolution. In this reference it was assumed that the intensity of the  $\omega$  meson-cluster coupling was proportional to the mass number of the light cluster and no coupling to the  $\sigma$ -meson was included.

The light clusters ( $d$ ,  $h$ ,  $t$  and  $\alpha$  particles) are treated as point like particles (without internal structure) within the RMF approximation. Just as the nucleons in nuclear matter, the clusters interact through the exchange of  $\sigma$ ,  $\omega$  and  $\rho$  meson fields. In order to understand how dependent are the results on the NLWM parametrization we consider three different parametrizations; NL3 [14], with a quite large symmetry energy and incompressibility at saturation and which was fitted in order to reproduce the ground state properties of both stable and unstable nuclei; FSU [15] and IU-FSU [16], which were accurately calibrated to simultaneously describe the GMR in  $^{90}\text{Zr}$  and  $^{208}\text{Pb}$ , and the IVGDR in  $^{208}\text{Pb}$  and still reproduce ground-state observables of stable and unstable nuclei. Furthermore, the IU-FSU was also refined to describe neutron stars with high masses ( $\sim 2M_\odot$ ).

In Ref. [1], where a generalized RMF model with density dependent couplings was developed including clusters as explicit degrees of freedom, the medium effects on the binding energy of the clusters were introduced explicitly through density and temperature dependent terms. We aim at getting a description of the light clusters in nuclear matter that is simpler to implement, yet more realistic than the excluded volume mechanism.

A brief review of the formalism is presented in section II, the results and discussion of the meson-cluster coupling constants are given in section III and conclusions are drawn in section IV.

## II. THE FORMALISM

We consider a system of protons and neutrons interacting with and through an isoscalar-scalar field  $\sigma$  with mass  $m_s$ , an isoscalar-vector field  $\omega^\mu$  with mass  $m_v$ , an isovector-vector field  $\mathbf{b}^\mu$  with mass  $m_\rho$  and light clusters:  $d$ ,  $h$ ,  $t$ , and  $\alpha$  particles. The Lagrangian density of this system reads:

$$\mathcal{L} = \sum_{j=p,n,t,h} \mathcal{L}_j + \mathcal{L}_\alpha + \mathcal{L}_d + \mathcal{L}_\sigma + \mathcal{L}_\omega + \mathcal{L}_\rho + \mathcal{L}_{\omega\rho},$$

where the Lagrangian  $\mathcal{L}_j$  is

$$\mathcal{L}_j = \bar{\psi}_j [\gamma_\mu i D_j^\mu - M_j^*] \psi_j, \quad (1)$$

with

$$i D_j^\mu = i \partial^\mu - g_v^j \omega^\mu - \frac{g_\rho^j}{2} \boldsymbol{\tau} \cdot \mathbf{b}^\mu, \quad (2)$$

$$M_j^* = M_j - g_s^j \sigma, \quad j = p, n, t, h \quad (3)$$

where  $M = (M_p + M_n)/2 = 938.918695 \text{ MeV}$ ,  $M_h = 3M - B_h$ ,  $M_t = 3M - B_t$ ,  $M_\alpha = 4M - B_\alpha$ ,  $M_d = 2M - B_d$ , with the binding energies given in Table I. The  $\alpha$  particles and the deuterons are described as in [1]

$$\mathcal{L}_\alpha = \frac{1}{2} (i D_\alpha^\mu \phi_\alpha)^* (i D_{\mu\alpha} \phi_\alpha) - \frac{1}{2} \phi_\alpha^* (M_\alpha^*)^2 \phi_\alpha, \quad (4)$$

$$\begin{aligned} \mathcal{L}_d = & \frac{1}{4} (i D_d^\mu \phi_d^\nu - i D_d^\nu \phi_d^\mu)^* (i D_{d\mu} \phi_{d\nu} - i D_{d\nu} \phi_{d\mu}) \\ & - \frac{1}{2} \phi_d^{\mu*} (M_d^*)^2 \phi_{d\mu}, \end{aligned} \quad (5)$$

where

$$i D_j^\mu = i \partial^\mu - g_v^j \omega^\mu \quad (6)$$

and

$$M_j^* = M_j - g_s^j \sigma \quad (7)$$

with  $j = \alpha, d$ . The meson Lagrangian densities are

$$\begin{aligned} \mathcal{L}_\sigma &= \frac{1}{2} \left( \partial_\mu \sigma \partial^\mu \sigma - m_s^2 \sigma^2 - \frac{1}{3} \kappa g_s^3 \sigma^3 - \frac{1}{12} \lambda g_s^4 \sigma^4 \right) \\ \mathcal{L}_\omega &= \frac{1}{2} \left( -\frac{1}{2} \Omega_{\mu\nu} \Omega^{\mu\nu} + m_v^2 \omega_\mu \omega^\mu + \frac{1}{12} \xi g_v^4 (\omega_\mu \omega^\mu)^2 \right) \\ \mathcal{L}_\rho &= \frac{1}{2} \left( -\frac{1}{2} \mathbf{B}_{\mu\nu} \cdot \mathbf{B}^{\mu\nu} + m_\rho^2 \mathbf{b}_\mu \cdot \mathbf{b}^\mu \right) \\ \mathcal{L}_{\omega\rho} &= \Lambda_v g_v^2 g_\rho^2 \omega_\mu \omega^\mu \mathbf{b}_\mu \cdot \mathbf{b}^\mu \end{aligned}$$

where  $\Omega_{\mu\nu} = \partial_\mu \omega_\nu - \partial_\nu \omega_\mu$ ,  $\mathbf{B}_{\mu\nu} = \partial_\mu \mathbf{b}_\nu - \partial_\nu \mathbf{b}_\mu - g_\rho (\mathbf{b}_\mu \times \mathbf{b}_\nu)$ . The parameters of the models are: the masses and the coupling parameters  $g_s$ ,  $g_v$ ,  $g_\rho$  of the mesons and  $\lambda$ ,  $\kappa$ ,  $\xi$ , and  $\Lambda_v$  of the nonlinear meson terms. In the above Lagrangian density  $\boldsymbol{\tau}$  is the isospin operator. When the NL3 parametrization is used,  $\xi$  and  $\Lambda_v$  are set equal to zero. The FSU and IU-FSU parametrizations include the nonlinear  $\omega\rho$  term.

The equations of motion in the relativistic mean field approximation for the meson fields are given by

$$\begin{aligned} m_s^2 \sigma + \frac{\kappa}{2} g_s^3 \sigma^2 + \frac{\lambda}{6} g_s^4 \sigma^3 &= \sum_{i=p,n,t,h} g_s^i \rho_s^i + \sum_{i=d,\alpha} g_s^i \rho_i \\ m_v^2 \omega^0 + \frac{1}{6} \xi g_v^4 (\omega^0)^3 + 2 \Lambda_v g_v^2 g_\rho^2 \omega^0 (b_3^0)^2 &= \sum_{i=p,n,t,h,d,\alpha} g_v^i \rho_i \\ m_\rho^2 b_3^0 + 2 \Lambda_v g_v^2 g_\rho^2 (\omega^0)^2 b_3^0 &= \sum_{i=p,n,t,h} g_\rho^i I_3^i \rho_i \end{aligned}$$

where,  $\rho_s^i$  is the scalar density given by

$$\rho_s^i = \frac{2S^i + 1}{2\pi^2} \int_0^{k_f^i} k^2 dk \frac{M_i - g_s^i \sigma}{\sqrt{k^2 + (M_i - g_s^i \sigma)^2}},$$

$\rho_i$  is the vector density,  $I_3^i$  ( $S^i$ ) is the isospin (spin) of the specie  $i$  for  $i = n, p, t, h$ . At zero temperature all the  $\alpha$  and deuteron populations will condense in a state of

zero momentum, therefore  $\rho_\alpha$  and  $\rho_d$  correspond to the condensate density of each specie.

The values of the parameters for each one of the relativistic effective interactions, discussed below, are in Table II and the corresponding properties of infinite nuclear matter at saturation density are shown in Table III.

TABLE I: Parameters for the cluster binding energy shifts defined in Eqs. (8)-(10) at  $T = 0$  MeV (taken from [1]).

Cluster $i$	$a_{i,1}$ (MeV $^{5/2}$ fm $^3$ )	$a_{i,2}$ (MeV)	$a_{i,3}$ (MeV)	$B_i^0$ [17] (MeV)
$t$	69516.2	7.49232	—	8.481798
$h$	58442.5	6.07718	—	7.718043
$\alpha$	164371	10.6701	—	28.29566
$d$	38386.4	22.5204	0.2223	2.224566

TABLE II: Parameter sets for the three models used in this work.

	NL3 [14]	FSU [15]	IU-FSU [16]
$m_s$ (MeV)	508.194	491.500	491.500
$m_v$ (MeV)	782.501	782.500	782.500
$m_\rho$ (MeV)	763.000	763.000	763.000
$g_s^2$	104.3871	112.1996	99.4266
$g_v^2$	165.5854	205.5469	169.8349
$g_\rho^2$	79.6000	138.4701	184.6877
$\kappa$ (MeV)	3.8599	1.4203	3.3808
$\lambda$	-0.015905	+0.023762	+0.000296
$\xi$	0.00	0.06	0.03
$\Lambda_v$	0.000	0.030	0.046

TABLE III: Bulk parameters characterizing the behavior of infinite symmetric nuclear matter at saturation density: the saturation density  $\rho_0$ , the binding energy  $E/A$ , the incompressibility  $K$ , the symmetry energy  $a_{sym}$  and its slope  $L$ , and the nucleon effective mass  $M^*$ .

	NL3	FSU	IU-FSU
$\rho_0$ (fm $^{-3}$ )	0.148	0.148	0.155
$E/A$ (MeV)	-16.24	-16.30	-16.40
$K$ (MeV)	271.5	230.0	231.2
$a_{sym}$ (MeV)	37.29	32.59	31.30
$L$ (MeV)	118.2	60.5	47.2
$M^*/M$	0.60	0.62	0.62

The total energy density is given by

$$\begin{aligned} \mathcal{E} = & \sum_{i=p,n,t,h} \left( \frac{2S^i + 1}{2\pi^2} \int_0^{k_f^i} k_i^2 dk_i \sqrt{k_i^2 + (M_i - g_s^i \sigma)^2} \right) \\ & + \sum_{i=p,n,t,h} (g_v^i \omega^0 \rho_i + g_\rho^i b_3^0 I_3^i \rho_i) + \frac{1}{2} m_s^2 \sigma^2 + \frac{1}{6} \kappa g_s^3 \sigma^3 \\ & + \frac{1}{24} \lambda g_s^4 \sigma^4 - \frac{1}{2} m_v^2 \omega_0 \omega^0 - \frac{1}{24} \xi g_v^4 (\omega^0)^4 - \frac{1}{2} m_\rho^2 (b_3^0)^2 \\ & - \Lambda_v g_v^2 g_\rho^2 \omega_0 \omega^0 (b_3^0)^2 + \sum_{i=\alpha,d} (M_i - g_s^i \sigma + g_v^i \omega^0) \rho_i. \end{aligned}$$

At zero temperature the free energy density  $\mathcal{F}$  and the energy density coincide.

We define the global proton fraction  $Y_p$  as

$$Y_p = \frac{\rho_p}{\rho} + 2 \frac{\rho_\alpha}{\rho} + \frac{\rho_d}{\rho} + 2 \frac{\rho_h}{\rho} + \frac{\rho_t}{\rho}.$$

where  $\rho = \rho_p + \rho_n + 4\rho_\alpha + 2\rho_d + 3\rho_h + 3\rho_t$  is the total baryonic density. Defining the mass fraction  $y_i = A_i(\rho_i/\rho)$  of the various species we obtain

$$Y_p = y_p + \frac{1}{2} y_\alpha + \frac{1}{2} y_d + \frac{2}{3} y_h + \frac{1}{3} y_t$$

for the global proton fraction.

### A. Cluster binding energy

In [1] using a quantum statistical approach, the following empirical quadratic form was proposed for the medium-dependent binding energy shift at zero temperature of the various clusters

$$\Delta B_i(\rho, T=0) = -\tilde{\rho}_i \left[ \delta B_i(0) + \frac{\tilde{\rho}_i}{2B_i^0} \delta B_i^2(0) \right] \quad (8)$$

where

$$\tilde{\rho}_i = \frac{2}{A_i} [Z_i \rho_p^{tot} + N_i \rho_n^{tot}].$$

The total nucleon density is given by  $\rho = \rho_p^{tot} + \rho_n^{tot}$  and

$$\delta B_i(T=0) = \frac{a_{i,1}}{a_{i,2}^{3/2}} \quad (9)$$

for  $i = t, h, \alpha$ , and

$$\delta B_d(T=0) = \frac{a_{d,1}}{2a_{d,3}^2 a_{d,2}^{3/2}} \quad (10)$$

for the deuteron. The parameters  $a_{i,1}$ ,  $a_{i,2}$  and  $a_{d,3}$ , taken from [1], are listed for symmetrical nuclear matter ( $Y_p = 0.5$ ) in Table I.

The density where a cluster becomes unbound,  $\rho_{dis}$ , referred as dissolution density, is given by

$$B_i(\rho_{dis}) = B_i^0 + \Delta B_i = 0. \quad (11)$$

The dissolution densities obtained for the light clusters considered at zero temperature and in symmetric nuclear matter are reported in the Table IV.

TABLE IV: Densities at which the clusters become unbound given by equation (11) for  $T = 0$  MeV.

	$t$	$h$	$\alpha$	$d$
$\rho_{dis} \text{ (fm}^{-3}\text{)}$	0.00183175	0.00144835	0.00439226	0.00044815

### III. RESULTS AND DISCUSSIONS

Our results will be reported in the present section. The calculations will all be performed at zero temperature except for Section III E where results at finite temperature will also be presented.

In the following we will consider each type of light clusters separately in order to study the dissolution density of each of them in nuclear matter.

We assume for the cluster couplings the form

$$\begin{aligned} g_v^j &= \eta_j g_v \\ g_s^j &= \beta_j g_s, \quad j = t, h, d, \alpha \\ g_\rho^i &= \delta_i g_\rho, \quad i = t, h, \\ g_\rho^i &= 0, \quad i = d, \alpha, \end{aligned} \quad (12)$$

where the parameters  $\eta_j$ ,  $\beta_j$  and  $\delta_i$  are constants. Next we determine the dissolution density ( $\rho_{dis}$ ) as a function of these parameters and study the dependence of  $\rho_{dis}$  on the global proton fraction ( $Y_p$ ). Experimental and theoretical information will be used to fix the parameters  $\eta_j$ ,  $\beta_j$  and  $\delta_i$ .

#### A. Simple choice of the coupling parameters

In order to have a feeling of the effect of including light clusters in the EOS, we will first fix the cluster coupling constants as  $g_s^i = 0$ ,  $g_v^i = A_i g_v$  for  $i = t, h, d, \alpha$  and  $g_\rho^h = g_\rho^t = g_\rho$  by fixing

$$\begin{aligned} \eta_j &= A_j, \quad \beta_j = 0, \quad j = d, t, h, \alpha, \\ \delta_i &= 1, \quad i = t, h, \\ \delta_i &= 0, \quad i = d, \alpha, \end{aligned} \quad (13)$$

in (12). This choice corresponds to the one used in [13, 20] and may be justified in the following way: a) since we do not know how nuclear matter affects the binding energy of the light clusters we take the  $\sigma$  coupling constants of the light clusters as zero ( $g_s^i = 0$ ); b) we expect that the  $\omega$  meson will play the role of an excluded volume, i.e., at large densities will hinder the superposition of clusters by giving rise to a repulsive contribution. We take the coupling  $g_v^i = A_i g_v$  and consider that this would be of the order of magnitude expected; c) we consider that the coupling of the light clusters to the  $\rho$  meson is defined by the corresponding cluster isospin.

The dissolution density at a given proton fraction and zero temperature is determined from the crossing be-

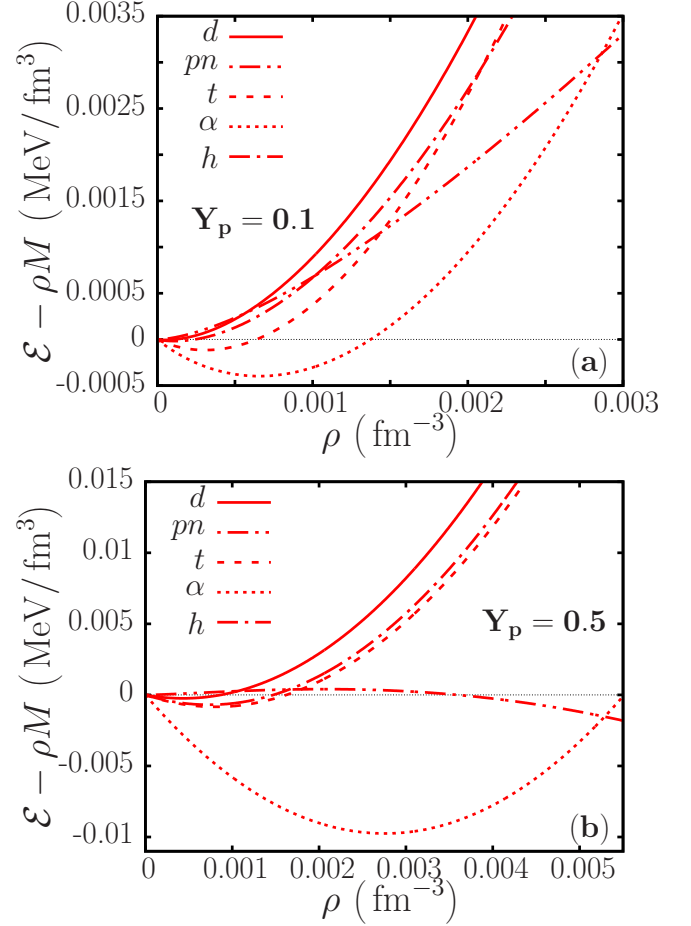


FIG. 1: (Color online) The free energy density minus the mass contribution at  $T = 0$  MeV as a function of the baryonic density for  $Y_p = 0.1$  (a) and  $Y_p = 0.5$  (b) for the FSU parametrization, with choice (13) for the cluster couplings. The EOS designed by the light cluster  $i$  has the largest possible fraction of clusters  $i$  and if, necessary, also protons and neutrons.

tween the proton-neutron free energy and the free energy of matter with the largest number of clusters it is possible to form. This is the most stable matter with clusters. The stable phase is the one with the lowest free energy density. At low densities the equilibrium phase is the cluster phase and at large densities it is the proton-neutron matter. In fact, from the Fig. 1 it is seen that this transition is characterized by a negative curvature of the free energy density, and therefore, it does not correspond to a thermodynamically stable phase transition. The inclusion of larger clusters is necessary to realistically describe this transition but this is not the aim of the present work.

The free energy density minus the mass contribution,  $\mathcal{F} = \mathcal{E} - M\rho$ , is plotted in Fig. 1 as a function of the baryon density for different EOS, namely the proton-neutron EOS without clusters and the proton-neutron matter with the largest possible fraction of one type of light cluster for the proton fractions considered ( $Y_p = 0.1$

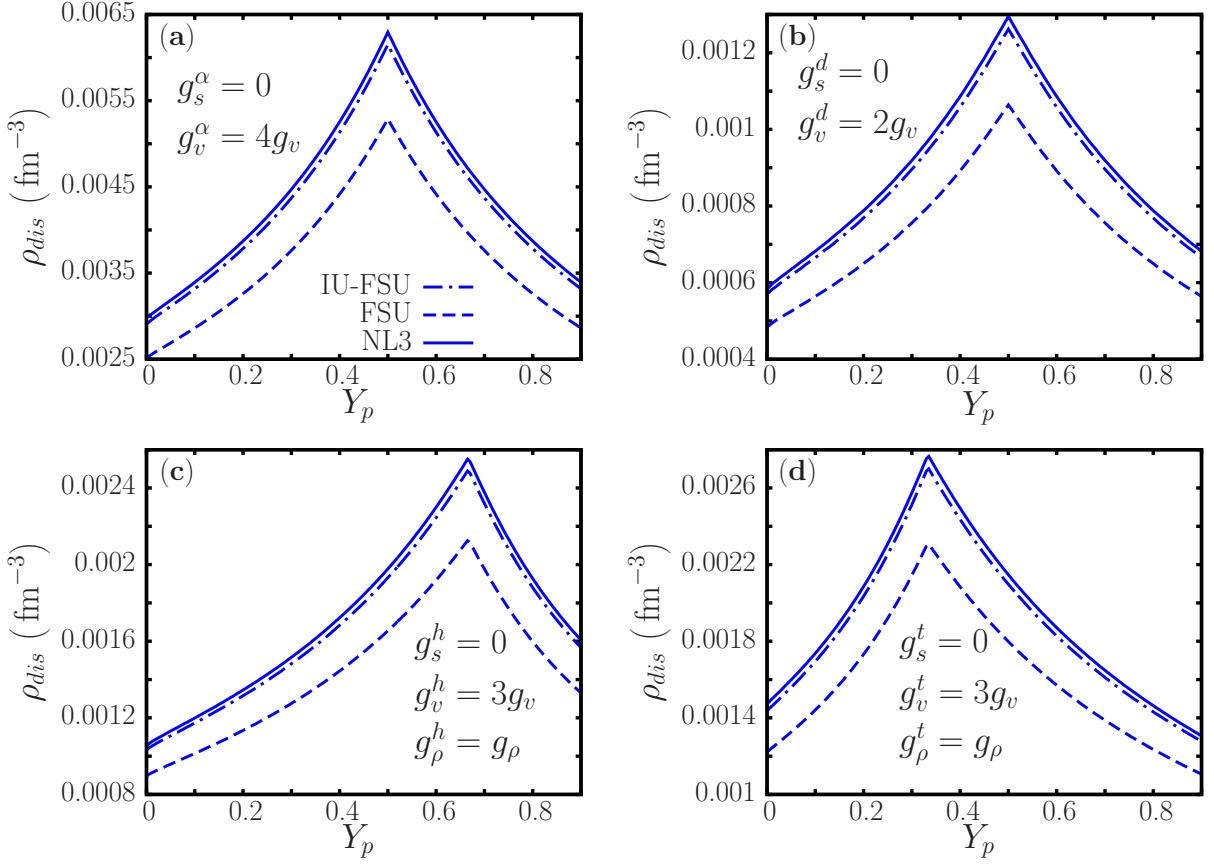


FIG. 2: (Color online) The dissolution density  $\rho_{dis}$  for  $T = 0$  MeV as a function of total proton fraction  $Y_p$  for the various clusters, with choice (13) for the cluster couplings:  $\alpha$  (a), deuterons (b), helions (c) and tritons (d). In each graph the curves represent NL3, IU-FSU and FSU from top to bottom, respectively.

and  $Y_p = 0.5$ ). The curves in Fig. 1 were obtained for FSU but for the other parametrizations the results are qualitatively the same. From Fig. 1 we see that there is some range of densities in which the free energy density of the equations of state with one type of cluster is lower than the pure nucleonic matter (without any bound states). In that range, the system can decrease its energy density by forming clusters. At  $T = 0$ , the EOS with  $\alpha$  particles is by far the most stable followed by the EOS with tritons, helions and deuterons. This sequence of stability is explained by the binding energy per nucleon of each cluster, having the  $\alpha$  particle the highest value and the deuteron the lowest one.

At finite temperature, all the clusters will be in chemical equilibrium and their abundances will be determined by a balance between temperature, their mass and binding energy.

The calculated dissolution densities are shown in Fig. 2 for all the clusters and the three NLW parametrizations with the choice (13) for the cluster couplings. For the deuteron and  $\alpha$  particles the maximum dissolution density is at  $Y_p = 0.5$  allowing the conversion of all nucleons into bound states (deuteron or  $\alpha$  particles). At  $Y_p = 2/3$  and  $Y_p = 1/3$ , all the nucleons are converted into he-

lions and tritons, respectively, giving the highest dissolution density. The NL3 and IU-FSU parametrizations give similar dissolution densities, with NL3 giving the highest ones. The IU-FSU parametrization gives results between FSU and NL3, very close to NL3, therefore, it will not be considered in most of the discussion and only the NL3 and FSU will be shown in the figures. The dissolution density of the light clusters within the different models is mainly determined by the isoscalar properties of the model. In particular, FSU has a quite large coupling constant to the  $\sigma$  meson which defines a smaller effective nucleon mass at low densities and, therefore, clusters will dissolve at smaller densities. This is also the reason why the NL3 dissolution density is the largest: for the densities of interest NL3 has the smallest nucleon effective mass.

We next generalize the choice (13) varying smoothly one parameter ( $\eta_i, \beta_i, \delta_i$ ) each time and keeping the other.



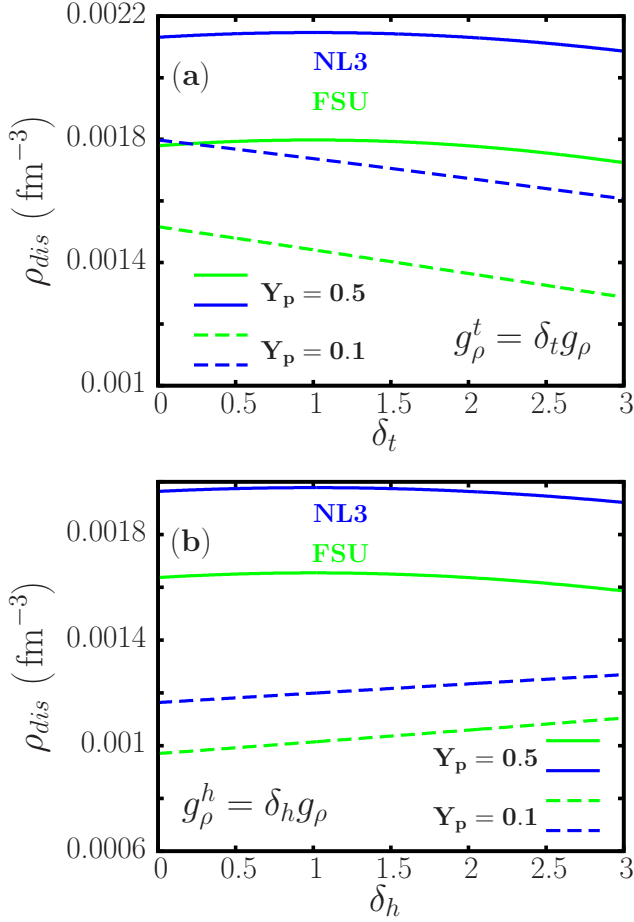


FIG. 3: (Color online) The dissolution density for tritons (a) and helions (b) as a function of  $\delta^i$  ( $g_\rho^i = \delta_i g_\rho$ ) for  $Y_p = 0.5$  (solid lines) and  $Y_p = 0.1$  (dashed lines).

### B. Varying the $g_\rho^i$ coupling constant

To study the effect of the  $\rho$  meson-cluster coupling constants  $g_\rho^i$  on the dissolution density for the helion and triton, we fix the other coupling constants by  $g_v^i = A_i g_v$  and  $g_s^i = 0$  and parametrize  $g_\rho^i$  by  $g_\rho^i = \delta_i g_\rho$  ( $i = h, t$ ). The results are shown in Fig. 3.

The densities of all species that are present are defined by the global proton fraction  $Y_p$ . For values of  $Y_p$  where only tritons and neutrons are present in nuclear matter, the free energy density term that depends on  $g_\rho^t$  is

$$\mathcal{F}(\delta_t) = \frac{1}{8} \frac{g_\rho^2}{(m_\rho^*)^2} (\delta_t \rho_t + \rho_n)^2 \quad (14)$$

and in the case where only helions and neutrons are present,

$$\mathcal{F}(\delta_h) = \frac{1}{8} \frac{g_\rho^2}{(m_\rho^*)^2} (\delta_h \rho_h - \rho_n)^2. \quad (15)$$

where  $(m_\rho^*)^2 = m_\rho^2 + 2g_\rho^2 g_v^2 \Lambda_v (\omega^0)^2$ .

Thus, for  $Y_p = 0.1$ , an increase in  $g_\rho^h$  through the parameter  $\delta_h$ , reduces the symmetry energy of a system composed by helions and consequently, the dissolution density increases. For a system made of tritons the opposite happens, and an increase in  $g_\rho^t$  increases the system symmetry energy leading to a decrease in the dissolution density.

For  $Y_p = 0.5$ , the helion and triton systems have a similar behavior, at some values of  $g_\rho^t$  and  $g_\rho^h$  they acquire the lowest free energy density, and consequently, the highest dissolution density due to the vanishing of the symmetry term, (14) or (15).

One important feature seen in Fig. 3 is the small range of variation of the dissolution density as a function of  $g_\rho^h$  and  $g_\rho^t$ , compared with the range of variation of the dissolution density as a function of the  $\omega$  and  $\sigma$  cluster coupling constants that we will discuss next. The cluster formation and dissolution is quite insensitive to the  $\rho$  meson-cluster coupling constant.

### C. Varying the $g_v^i$ coupling constant

The effect of the  $\omega$ -cluster coupling constants on the dissolution density is studied by fixing the  $\sigma$  and  $\rho$  coupling constants as  $g_s^i = 0$  ( $i = t, h, d, \alpha$ ) and  $g_\rho^i = g_\rho$  ( $i = t, h$ ). The  $g_v^i$  is parametrized by  $\eta_i$  as  $g_v^i = \eta_i g_v$ . The dissolution density versus  $\eta_i$  for all the clusters is shown in Fig. 4 for symmetric ( $Y_p = 0.5$ ) and asymmetric ( $Y_p = 0.1$ ) nuclear matter.

An increase in  $g_v^i$  decreases the dissolution density for all clusters. This is due to the fact that an increase in  $g_v^i$  leads to a more intense repulsion between the clusters, thus favoring their dissolution.

For  $Y_p = 0.1$  the dissolution density is lower than for  $Y_p = 0.5$ . This was expected because for  $Y_p = 0.1$  the number of clusters that can be formed is smaller than for symmetric nuclear matter. To dissolve a bigger number of clusters we need a bigger amount of energy and, thus, makes the cluster states with  $Y_p = 0.5$  more stable than  $Y_p = 0.1$ .

### D. Varying the $g_s^i$ coupling constant

To study the dissolution density dependence on the  $\sigma$ -cluster coupling constants of all clusters  $g_s^i$  we fix the  $\omega$  and  $\rho$  coupling constants as  $g_\rho^i = g_\rho$  ( $i = t, h$ ) and  $g_v^i = A_i g_v$  ( $i = t, h, d, \alpha$ ) and parametrize  $g_s^i$  as  $g_s^i = \beta_i g_s$ .

The results are shown in Fig. 5 for  $Y_p = 0.5$  and  $Y_p = 0.1$ . As expected the dissolution density grows as the  $g_s^i$  increases. An increase in  $g_s^i$  makes the cluster more bound (smaller effective mass) and, therefore, cluster states become more stable. Except for the helion, in all other cases for a given value of  $\beta$ , the dissolution densities of the clusters become larger for  $Y_p = 0.1$  than

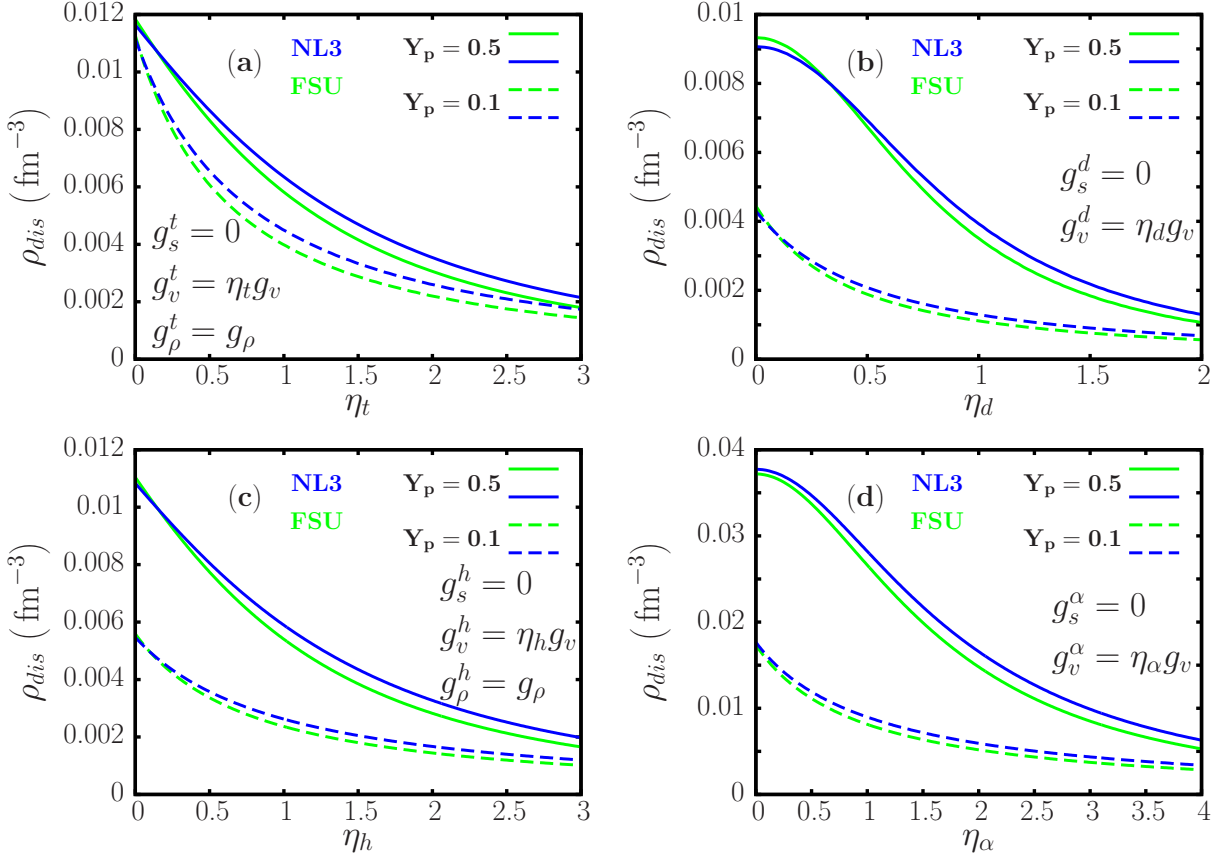


FIG. 4: (Color online) Dissolution density of each cluster as a function of  $\eta_i$  ( $g_v^i = \eta_i g_v$ ) for  $Y_p = 0.5$  (solid lines) and  $Y_p = 0.1$  (dashed lines): tritons (a), deuterons (b), helions (c) and  $\alpha$  (d).

$Y_p = 0.5$ . This is because when considering  $Y_p = 0.5$  we are comparing matter with clusters with nuclear symmetric matter, that is nuclear matter in its most bound state. For  $Y_p = 0.1$  nuclear matter is not even bounded. Increasing the binding energy of the clusters will stabilize them more relatively to the homogeneous asymmetric nuclear matter than in the previous case to symmetric matter. For helions there are too few clusters in matter with  $Y_p = 0.1$  and therefore the curves  $Y_p = 0.5$  and  $0.1$  will never cross.

When  $\beta_i$  is well below  $A_i$ , the dissolution density slightly changes for all clusters. For some value of  $\beta_i$  below  $A_i$  the dissolution density increases abruptly and the system becomes absolutely stable, in other words, the clusters will not dissolve for any density.

### E. A physical choice for the cluster coupling constants

After analyzing the effect of the different cluster-meson couplings, we discuss how these couplings could be fixed taking into account theoretical many-body calculations and experimental information.

To fix the  $\sigma$  and  $\omega$  clusters couplings two constraints

are required for each cluster. We consider the dissolution densities for symmetric nuclear matter at  $T = 0$  MeV given in Ref. [2] and shown in Table IV. However, this information is not enough to completely fix the cluster-meson couplings and we can find several sets of coupling constants that reproduce the dissolution densities. Therefore, we choose to fix two coupling constants for each cluster and fit the remaining to reproduce its dissolution density, namely, we fix  $g_s^i$  and  $g_\rho^i$ . For  $g_s^i$  we take several values,  $0$ ,  $A_i/2 g_s$ ,  $3A_i/4 g_s$ ,  $4A_i/5 g_s$ , for all clusters and for  $g_\rho^i$  we consider  $g_\rho^i = g_\rho$ ,  $\delta_i = 1$ , for triton and helion, and  $g_\rho^i = 0$ ,  $\delta_i = 0$ , for the isospin symmetric clusters, which is a reasonable choice, and, as we have shown, this coupling does not affect much the dissolution density of the cluster. Then, for each choice of  $g_s^i$ ,  $g_v^i$  is fit to reproduce the dissolution density of each cluster. The calculated values are shown in Table V. Different choices of  $g_s^i$ , together with the above restriction for  $g_v^i$ , will allow us to discuss the effect of this coupling constant on the overall particle fraction. In general we should have a different ratio  $g_s^i/g_s$  for each cluster, but, to simplify the discussion, we take the same for all clusters.

The relative magnitude of the  $\omega$ -cluster coupling of the different models is related to the  $\omega$ -nucleon coupling constant  $g_v$ : the smaller the values of  $g_v$  the larger the

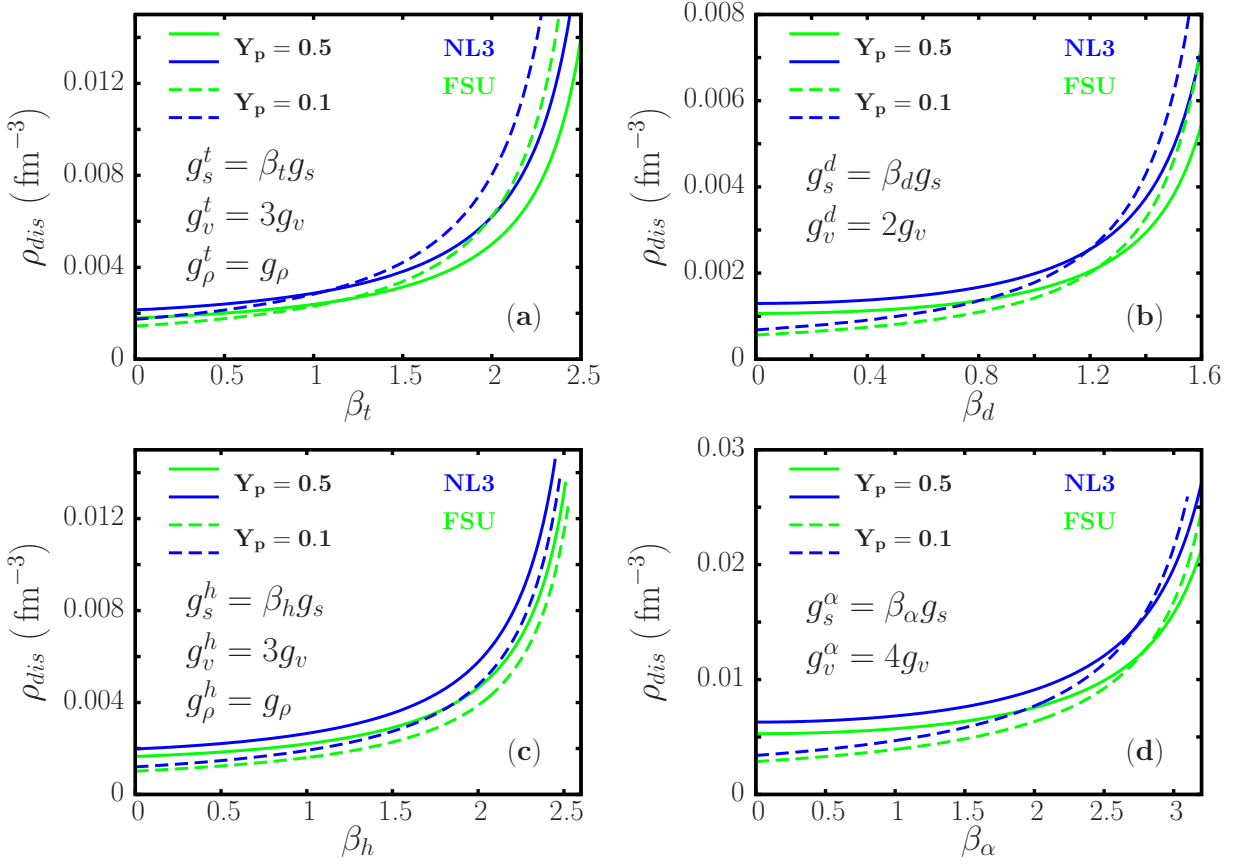


FIG. 5: (Color online) Dissolution density of each cluster as a function of  $\beta_i$  ( $g_s^i = \beta_i g_s$ ) for  $Y_p = 0.5$  (solid lines) and  $Y_p = 0.1$  (dashed lines): tritons (a), deuterons (b), helions (c) and  $\alpha$  (d).

$\omega$ -cluster coupling fractions  $g_v^i/g_v$ , and the difference between  $g_v^i$  for the models used is around 1%. In fact, for example, we find that for  $g_s^i = 0$ ,  $g_v^i$  is 43.22 (NL3), 42.40 (FSU) and 42.92 (IU-FSU).

More experimental information is needed in order to determine the coupling constants of the phenomenological model we propose. Recently, in-medium binding energies and Mott points of  $d$ ,  $t$ ,  $h$  and  $\alpha$  clusters have been determined experimentally [19]. For each cluster a combination of density and temperature corresponding to a vanishing in-medium cluster binding energy, the Mott point, were determined in a temperature range close to  $T = 5$  MeV. These results, together with the dissolution densities at  $T = 0$  MeV given in Table IV, will be used to determine the cluster coupling constant  $g_s^i$ .

In the study by Typel *et al.* [1] the binding energy of the clusters in the medium,

$$B_i = A_i M^* - M_i^* \quad (16)$$

where  $M_i^*$  is the effective mass of cluster  $i$  defined in (3) and (7), was parametrized as a function of density and temperature. In Fig. 6(a) we compare the in-medium binding energy of the  $\alpha$ -clusters as a function of the density for several values of the couplings  $g_s^i$ . All results were obtained at  $T = 5$  MeV but, in fact, they do not

depend much on the temperature. In the same figure we also include results obtained in [1] at  $T = 5$  MeV, which turn out to be very close to the calculated binding energies settings  $g_s^i = 3 A_i/4 g_s$ . In order to reproduce the results of [1] we must consider temperature dependent  $\sigma$ -cluster. We note, however, that choosing a temperature dependent parameter will alter the usual thermodynamic relations between energy density and pressure. In Fig. 6(b) we compare the in-medium binding energy of the four light clusters obtained in our calculation setting  $g_s^i = 3 A_i/4 g_s$  with the results of [1]: the best accordance occurs for the  $\alpha$ -clusters. We may get a better accordance for all the clusters if a different coupling fraction  $g_s^i/g_s$  is taken for each cluster.

In Fig. 7 we compare the Mott densities, the densities at which the binding energies defined in (16) vanish, at  $T = 5$  setting  $g_s^i = 3 A_i/4 g_s$  (open triangles) with the experimental Mott points determined in [19] (full dots with errorbars) and the parametrization of the Mott point given in [1] (dashed lines). Results in [19] are obtained at different temperatures for the four light clusters, however, all temperatures lie close to 5 MeV. We conclude that choosing  $g_s^i = 3 A_i/4 g_s$ , and the corresponding  $g_v^i$  and  $g_\rho^i$  couplings defined in Table V, at  $T = 5$  MeV in our model, gives results that are in rea-



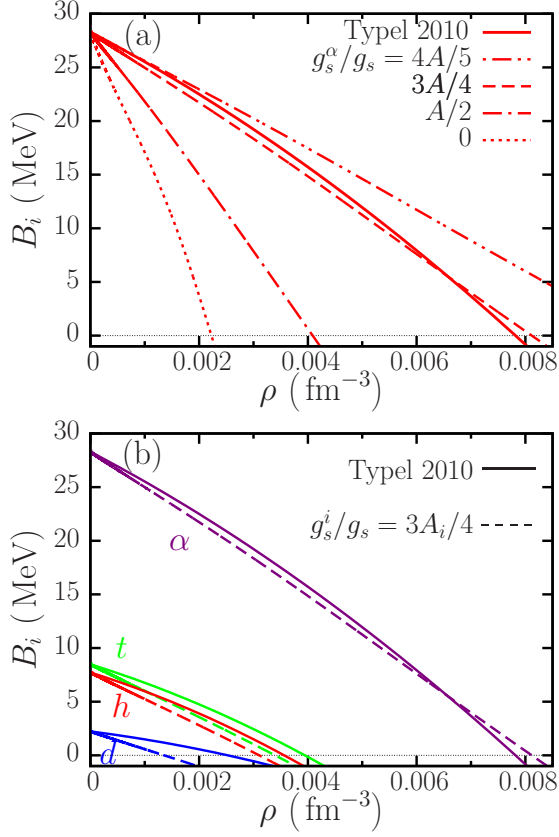


FIG. 6: (Color online) Binding energy, as defined in Eq. (16), of light clusters in equilibrium with symmetric nuclear matter described within FSU at  $T = 5$  MeV. In (a) the binding energy of  $\alpha$ -particles is given for several values of the coupling  $g_{s\alpha}$  (dashed, dotted and dash-dotted curves). The  $\alpha$  in-medium binding energy given in Typel 2010 [1] for  $T = 5$  MeV is also included (full line). In (b) we consider  $g_s^i = 3A_i/4g_s$  for all the clusters (dashed lines) and compare with the corresponding results of Typel 2010 [1] at  $T = 5$  MeV (full lines).

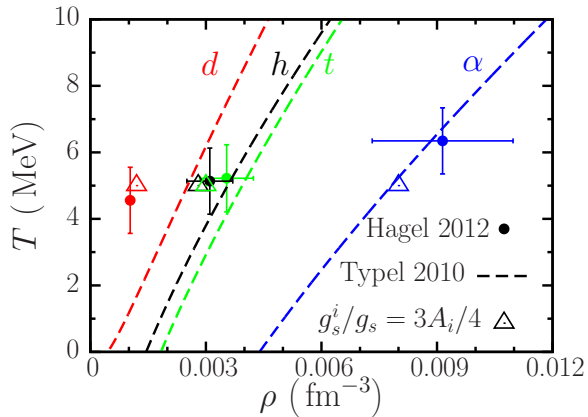


FIG. 7: (Color online) The Mott density for different temperatures and light clusters: results from Typel 2010 [1] (dashed lines), experimental prediction by Hagel 2012 [19] (full dots with errorbars), results for  $g_s^i/g_s = 3A_i/4$  and  $T = 5$  MeV (open triangle).

TABLE V: Cluster coupling constants  $g_v^i$  obtained for symmetric matter ( $Y_p = 0.5$ ) that reproduce the dissolution densities of Table IV, for several values of the coupling  $g_s^i$ .  $g_\rho^i/g_\rho = 1$  for the triton and the helion and zero for the deuteron and the  $\alpha$ .

$g_s^i/g_s$	$g_v^i/g_v$				
	0	$A_i/2$	$2A_i/3$	$3A_i/4$	$4A_i/5$
FSU					
$t$	2.961	3.793	4.177	4.382	4.509
$h$	3.283	4.064	4.428	4.624	4.745
$d$	3.038	3.260	3.422	3.516	3.577
$\alpha$	4.440	5.027	5.439	5.675	5.824
NL3					
$t$	3.357	4.172	4.559	4.765	4.892
$h$	3.718	4.485	4.847	5.043	5.164
$d$	3.371	3.585	3.744	3.837	3.897
$\alpha$	4.919	5.491	5.897	6.131	6.278
IUFSU					
$t$	3.303	4.126	4.508	4.715	4.842
$h$	3.658	4.429	4.792	4.988	5.110
$d$	3.327	3.543	3.702	3.796	3.859
$\alpha$	4.854	5.429	5.837	6.071	6.220

sonable agreement with the data of Ref. [19] for the Mott density.

As a test of the parametrizations proposed for  $g_s^i = 3A_i/4g_s$  in Table V, we calculate the particle fraction at finite temperature and in chemical equilibrium,  $\mu_i = Z_i\mu_p + (A_i - Z_i)\mu_n$  with  $i = \alpha, h, t, d$  [13, 20]. We first focus on the effect of  $g_s^i$  and show in Fig. 8(a) the fraction of light clusters at  $T = 5$  for symmetric nuclear matter obtained for two values of the  $\sigma$ -cluster coupling constant, 0 (dashed lines) and  $3A_i/4g_s$  (full lines). It is seen that the particle fraction and dissolution density is sensitive to this coupling: for a larger coupling, both the fraction of particles and the dissolution density are larger. In Figs. 8(b) – 8(d), we always set  $g_s^i = 3A_i/4g_s$ . In Fig. 8(b) we compare two models, NL3 (dashed lines) and FSU (full lines). It is seen that the results do not differ much except for the deuterons that dissolve at a larger density and attain a larger fraction with NL3. At very low densities when the interaction between nucleons and clusters is negligible both models coincide; at densities just below the dissolution density, where models differ the most, the differences are not very large. The effect of temperature and isospin asymmetry is shown in Fig. 8(c) and (d). In Fig. 8(c) particle fractions in symmetric matter are compared for  $T = 10$  MeV (full lines) and  $T = 5$  MeV (dashed lines). At  $T = 10$  MeV the deuteron fraction is already the largest fraction and the  $\alpha$  fraction the smallest. In neutron rich matter, such as the one represented in 8(d), the deuteron fraction is the largest and the tritons come in second both at  $T = 5$  and 10 MeV.

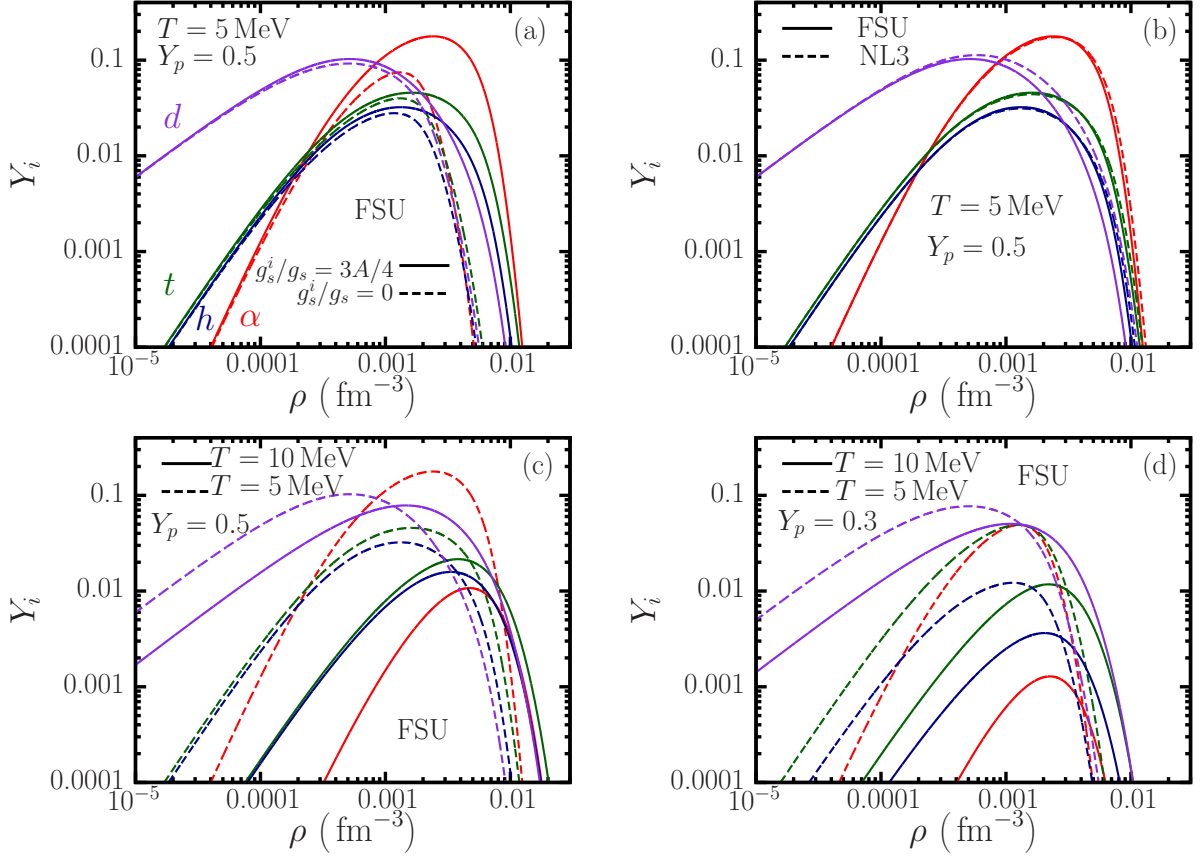


FIG. 8: (Color online) Fraction of light clusters in equilibrium with nuclear matter: (a) for FSU with  $Y_p = 0.5$  and  $T = 5$  MeV, and  $g_s^i = 0$  (dashed lines) and  $g_s^i = 3A_i/4g_s$  (full lines); (b) for  $g_s^i = 3A_i/4g_s$  with  $Y_p = 0.5$  and  $T = 5$  MeV and FSU (full lines) and NL3 (dashed lines); (c) for FSU with  $g_s^i = 3A_i/4g_s$  and  $Y_p = 0.5$ , and  $T = 10$  MeV (full lines) and  $T = 5$  MeV (dashed lines); (d) for FSU with  $g_s^i = 3A_i/4g_s$  and  $Y_p = 0.3$ , and  $T = 10$  MeV (full lines) and  $T = 5$  MeV (dashed lines).

The large amount of deuterons is in agreement with results of [18], where composition of low-density supernova matter composed of light nuclei was calculated within a quasiparticle gas model, and [3], where composition of the outer layers of a protoneutron star was studied.

#### IV. CONCLUSIONS

In the present work we have included light clusters in the EOS of nuclear matter within the framework of relativistic mean field models with constant coupling constants. Clusters are considered point-like particles that interact with the nucleons through the exchange of mesons. The formation of clusters is favorable at a quite low density; below  $0.002 \text{ fm}^{-3}$ , we expect that it is a reasonable approximation to consider them as point like.

It was shown that the dissolution of clusters is mainly determined by the isoscalar part of the EOS. Therefore, the  $\rho$ -cluster coupling constant was simply determined by the isospin of the cluster. To fix the  $\sigma$  and  $\omega$  clusters couplings two constraints are required for each cluster. In the present work we have considered the dissolution

density obtained in a quantum statistical approach [4] as a constraint to fix the  $\omega$ -cluster coupling. Recent experimental results for the in-medium binding energy of light clusters [19] allow the determination of the  $\sigma$ -cluster coupling strength at  $T \sim 5$  MeV. The virial expansion of the EOS at low densities and finite temperature is another constraint that could be used to fix the  $\sigma$ -meson coupling and that will be investigated.

We have applied the couplings proposed within the present to study symmetric and asymmetric nuclear matter with light clusters in chemical equilibrium at finite temperature and we have determined the relative light cluster fractions at  $T = 5$  MeV and  $T = 10$  MeV. It was shown that a larger  $\sigma$ -cluster coupling gives rise to larger dissolution densities and larger particle fractions.

The experimental determination of Mott points at more temperatures than the ones obtained in [19] would allow the determination of the temperature dependence. A comparison of the in-medium binding energies obtained within the present model with the ones proposed in [1], indicate that the last may be reproduced if temperature dependent meson-cluster couplings are obtained. It was shown that deuterons and tritons are the clus-

ters with larger abundances in asymmetric matter above  $T = 5$  MeV.. The results do not depend much on the RMF interaction chosen.

**Acknowledgments:** This work was partially sup-

ported by QREN/FEDER, the Programme COMPETE, under the project PTDC/FIS/113292/2009 and by Compstar, an ESF Research Networking Programme.

- 
- [1] S. Typel, G. Röpke, T. Klahn, D. Blaschke and H.H. Wolter, Phys. Rev. C **81**, 015803 (2010).
  - [2] G. Röpke, Phys. Rev. C **79**, 014002 (2009).
  - [3] A. Arcones, G. Martinez-Pinedo, E. O'Connor, A. Schwenk, H.-T. Janka, C. J. Horowitz, and K. Langanke, Phys. Rev. C **78**, 015806 (2008).
  - [4] M. Beyer, S.A. Sofianos, C. Kuhrtz, G. Röpke and P. Schuck, Phys. Lett. B **488**, 247 (2000).
  - [5] J. M. Lattimer and F. D. Swesty, Nucl. Phys. A **535**, 331 (1991).
  - [6] H. Shen, H. Toki, K. Oyamatsu, K. Sumiyoshi, Nucl. Phys. A **637**, 435 (1998).
  - [7] C.J. Horowitz and A. Schwenk, Nucl. Phys. A **776**, 55 (2006).
  - [8] E. O'Connor, D. Gazit, C. J. Horowitz, A. Schwenk, and N. Barnea, Phys. Rev. C **75**, 055803 (2007).
  - [9] Matthias Hempel, Jürgen Schaffner-Bielich, Stefan Typel, and Gerd Röpke, Phys. Rev. C **84**, 055804 (2011)
  - [10] M. Hempel and J. Schaffner-Bielich, Nucl. Phys. A **837**, 210 (2010).
  - [11] B. Serot and J. D. Walecka, Adv. Nucl. Phys. **16**, 1 (1986); J. Boguta and A. R. Bodmer, Nucl. Phys. A **292**, 413 (1977).
  - [12] G. Röpke, Nucl. Phys. A **867**, 66 (2011).
  - [13] S. S. Avancini, C. C. Barros, Jr., D. P. Menezes, and C. Providência, Phys. Rev. C **82**, 025808 (2010)
  - [14] G. A. Lalazissis, J. König and P. Ring, Phys. Rev. C **55**, 540 (1997).
  - [15] B. G. Todd-Rutel and J. Piekarewicz, Phys. Rev. Lett. **95**, 122501 (2005).
  - [16] F. J. Fattoyev, C. J. Horowitz, J. Piekarewicz and G. Shen, Phys. Rev. C **82**, 055803 (2010).
  - [17] G. Audi, A. H. Wapstra and C. Thibault, Nucl. Phys. A **729**, 337 (2002).
  - [18] S. Heckel, P. P. Schneider, and A. Sedrakian, Phys. Rev. C **80**, 015805 (2009).
  - [19] K. Hagel *et al.*, Phys. Rev. Lett. **108**, 062702 (2012)
  - [20] S. S. Avancini, C. C. Barros, Jr., L. Brito, S. Chiacchiera, D. P. Menezes, and C. Providência, Phys. Rev. C **85**, 035806 (2012).